Inverse Magnetoresistance in Magnetic Tunnel Junction With an Fe_3O_4 Electrode

Chando Park, Jian-Gang Zhu, Yingguo Peng, David E. Laughlin, and Robert M. White

Data Storage System Center, Carnegie Mellon University, Pittsburgh, PA 15213

Magnetic tunnel junctions (MTJ) with a plasma-oxidized Fe electrode have been fabricated on oxidized silicon wafers with standard photolithography. High-resolution transmission electron microscopy (HRTEM) and diffraction patterns show that a thin Fe layer can be oxidized by a controlled oxygen plasma into pure Fe_3O_4 without other crystallographic phases such as FeO and Fe_2O_3. To grow Fe_3O_4 directly in contact with an AlOx barrier, we began with Fe layers that varied from 1.8 to 5 nm. It was found that complete oxidation only occurred for the 1.8-nm thickness. Magnetic and electrical transport properties on the MTJs were measured at room temperature and low temperature (110 K). When the layer adjacent to the AlOx barrier was Fe_3O_4, inverse magnetoresistance (MR) behavior was observed, which is what is expected from the band structure of Fe_3O_4. However, when free Fe exists due to incomplete oxidation, positive MR behavior is observed.

Index Terms—**Half-metal, magnetite, magnetic tunnel junction (MTJs), magnetoresistance ratio.**

I. Introduction

As a result of their high spin polarization (100%), half-metallic materials having only one spin-subband at the Fermi level are very attractive as electrodes in magnetic tunnel junctions (MTJ). From the band calculation, Fe_3O_4 (magnetite) is one of the half metals which has an energy gap in the majority spin band at the Fermi level [1]. Only for spindown electrons, are there available states at the Fermi level which means that the conduction electrons have spin down, i.e., $P = -100\%$. Experimental data shows that the spin polarization near the Fermi energy E_F is—$(80 \pm 5)\%$ [2]. In general, most ferromagnets such as NiFe and CoFe, with AlOx tunnel barrier show a positive spin polarization [3]. Since Fe_3O_4 has a negative spin polarization, the expected magnetoresistance (MR) for a tunnel junction with the ferromagnet and Fe_3O_4 electrorodes should show an inverse MR according to Julières equation [4]. MTJs with a Fe_3O_4 electrode has been studied by several groups. Seneor *et al.* [5] fabricated magnetic tunnel junctions using Co as one electrode and iron oxide (mixture of Fe_3O_4 and γ-Fe_2O_3) as the other electrode with AlOx barrier. These MTJs showed a tunneling magnetoresistance (TMR) of 13% at room temperature. Wang *et al.* [6] reported a TMR of 14% at room temperature using CoFe and Fe_3O_4 with an AlOx barrier. But these TMRs were all positive. Recently polycrystalline Fe_3O_4 based tunnel junctions (Fe_3O_4/AlOx/CoFe) and epitaxial Fe_3O_4 based tunnel junctions ($Fe_3O_4/CoCr_2O_3/La_{0.7}Sr_{0.3}MnO_3$) have shown an inverse TMR of -15% and the junction magnetoresistance (JMR) of -0.5% at room temperature, respectively [7], [8]. However, the origin of the sign of the MR for these tunnel junctions remains unclear. Through the experimental results presented in the rest of this paper, we shall show a NiFe/AlOx/Fe_3O_4 tunnel junction does indeed have inverse MR if sufficiently pure Fe_3O_4 at the interface with the tunnel barrier can be achieved.

II. Experimental Procedures

Magnetic tunnel junctions with the structure of Ta 3/Cu 50/Ta 3/NiFe 10/AlOx 2/Fe (1.8–10 nm) + oxidation/Fe 5/Ta 3 were deposited on oxidized silicon substrates by using an RF/dc sputtering system. All our junctions were patterned by photolithography and ion beam etching. Junction size varied from 4×4 μm^2 to 16×16 μm^2. The tunnel barrier layer was formed by plasma oxidation of 1.7 nm of Al for 45 s. For the Fe_3O_4, we first deposited an Fe layer on top of the AlOx and subsequently oxidized the Fe with an oxygen plasma. This process requires careful control of the plasma condition and the Fe layer thickness such that all the Fe adjacent to AlOx layer is converted into Fe_3O_4. On top of the oxidized Fe layer, another Fe layer was deposited to ensure lateral ferromagnetic coupling through the layer. The Fe layer also prevents the Fe_3O_4 layer from being reduced [9], [10]. The microstructures of the films were investigated by high resolution transmission electron microscopy (HRTEM), and conventional TEM. The magnetic properties were measured using a vibrating sample magnetometer (VSM) with fields up to 350 Oe. The magntoresistance (MR) transfer curve was measured by a four point measurement with fields up to 350 Oe.

III. Results and Discussion

Fig. 1 shows (a) cross section TEM and (b) HRTEM images of the structure of Ta 3/NiFe 10/AlOx 2/Fe 10 nm $+O_2$ plasma/Fe 5/Ta 3 nm. To identify the phases, we measured the d-spacings from the fast Fourier transformation (FFT)of the high-resolution image [9], [11]. As shown in the Fig. 1(b), in the oxidized Fe layer, only the top 2 nm of the Fe layer has transformed into a 3.3–3.5-nm-thick Fe_3O_4 layer. The remaining 8 nm remains Fe. Apparently, 3.3–3.5 nm Fe_3O_4 layer effectively passivates the rest of the Fe layer. This indicates that to ensure a complete Fe_3O_4 layer to form at the interface with the AlOx tunnel barrier, the Fe layer to be oxidized needs to be thinner than 2 nm in this method.

The Fe_3O_4 layer formed from the oxidized Fe layer is also identified in the electron diffraction pattern of the plan

Digital Object Identifier 10.1109/TMAG.2005.855294

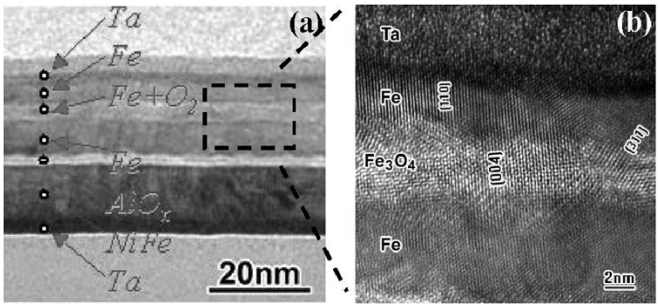

Fig. 1. Cross-section TEM (a), and HRTEM images (b) of the structure of Ta 3/NiFe 10/AlOx 2/Fe 10 nm + O_2 plasma/Fe 5/Ta 3 nm.

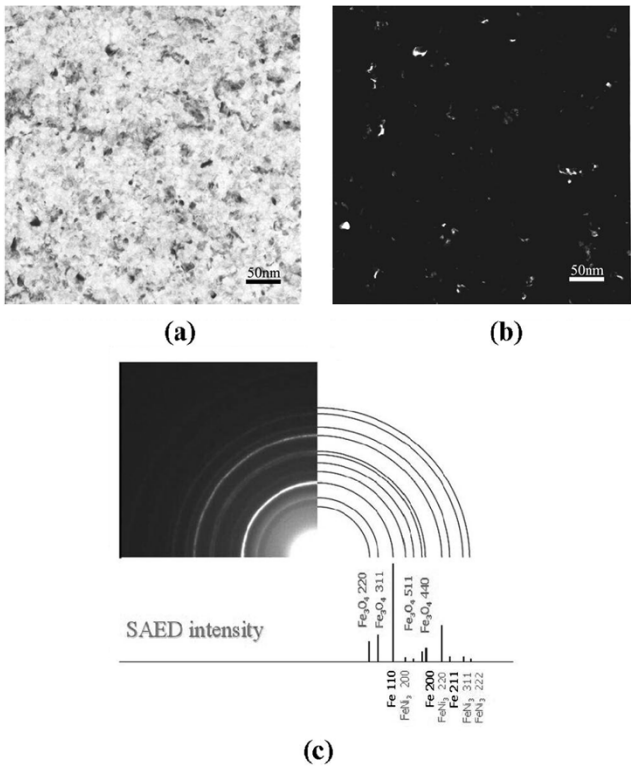

Fig. 2. (a) Bright-field and (b) dark-field images and (c) selected area electron diffraction pattern of the Fe_3O_4 layer in the structure of Ta 3/Cu 50/Ta 3/NiFe 10/AlOx 2/Fe 2.5 nm + O_2 plasma/Fe 5/Ta 3 nm.

view TEM image of the Fe_3O_4 layer in the structures of Ta 3/NiFe10/AlOx 2/Fe2.5 nm+O_2 plasma/Fe 5/Ta 3 nm, as shown in Fig. 2(c). To make a sample for the TEM plan view image of the Fe_3O_4 layer, an ion milling step was precisely controlled to produce a thin area of the Fe_3O_4 layer in a sample with multilayers, as described in a previous paper [12]. The diffraction rings clearly indicate the Fe_3O_4 phase along with Fe and $FeNi_3$ phases that are associated with the top and the bottom electrode, respectively. The diffraction rings show no Fe_2O_3 or FeO phases, consistent with HRTEM analysis. The bright-field and dark-field images [Fig. 2(a) and (b)] show grain sizes in the range of 5–10 nm with no apparent texture.

Since the oxidation penetration depth is only about 2 nm in the oxidized Fe layer, the Fe layer thickness was systematically reduced. Fig. 3 shows measured MR transfer curves for the Fe layer thicknesses of 5, 2.5, 2, and 1.8 nm. The junction size was $16 \times 12\ \mu m^2$. The same oxidation condition was applied after

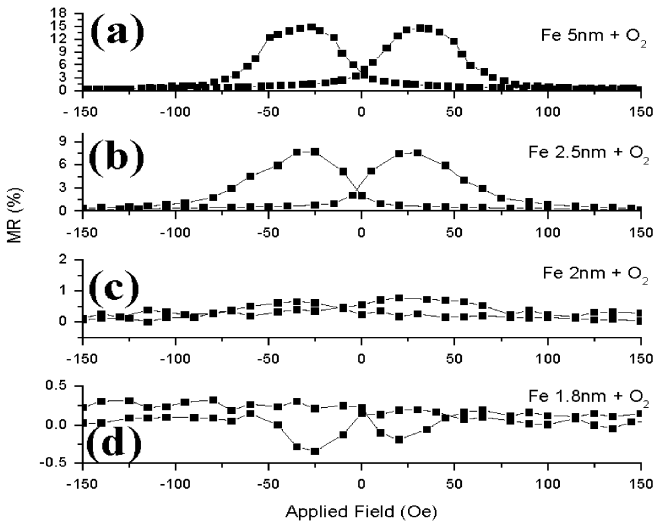

Fig. 3. Magnetoresistance transfer curve of junction structure of Ta 3/Cu 50/Ta 3/NiFe 10/AlOx 2 nm/Fe [(a) 5, (b) 2.5, (c) 2, and (d) 1.8 nm] + O_2 plasma/Fe 5/Ta 3 nm.

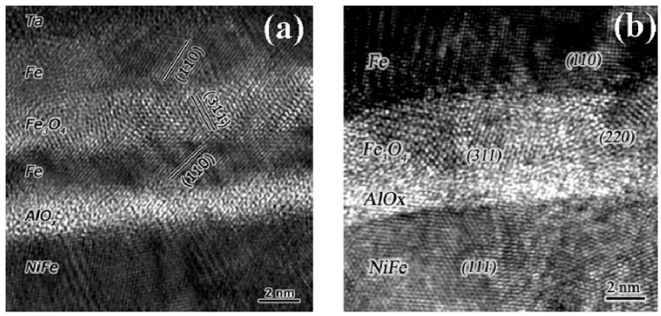

Fig. 4. Cross section HRTEM images of junction structure of Ta 3/Cu 50/Ta 3/NiFe 10/AlOx 2/Fe [(a) 5 and (b) 1.8 nm] + O_2 plasma/Fe 5/Ta 3 nm.

each Fe layer deposition. With a 5-nm Fe layer thickness, the magnetoresistance is positive and exhibits a similar value as if the electrode is pure Fe. However, when the Fe layer thickness is reduced below 2.5 nm, the measured MR value starts to decrease. At 2-nm thickness, the MR value becomes essentially zero. When the Fe layer thickness is 1.8 nm, the MR curve becomes negative (inverse), the parallel state having the highest resistance while the antiparallel state has the lowest resistance. At this thickness, the Fe layer has essentially completely transformed into Fe_3O_4 as shown in Fig. 4(b). At the tunnel barrier interface, the polycrystalline Fe_3O_4 phase dominates. For the 2 nm thick Fe layer case, an unoxidized residual Fe phase coexists with the Fe_3O_4 phase, resulting in zero MR.

Fig. 4 shows cross section HRTEM images of tunnel junctions formed from 5-nm-thick Fe (thickness before the oxidation) and 1.8-nm thickness Fe. When the Fe thickness was 5 nm, 2 nm of unoxidized Fe layer remained next to the AlOx barrier as we expected from the HRTEM analysis in Fig. 1(b). When the Fe thickness was 1.8 nm, the Fe layer was fully oxidized which means that the Fe_3O_4 is directly in contact with AlOx barrier. Based on our MR and TEM results, we conclude that the interface phase between AlOx barrier and Fe_3O_4 determines the MR behavior. Many previous publications showed positive MR for ferromagnet/AlOx/Fe_3O_4 tunnel junctions [5], [6]. Our results

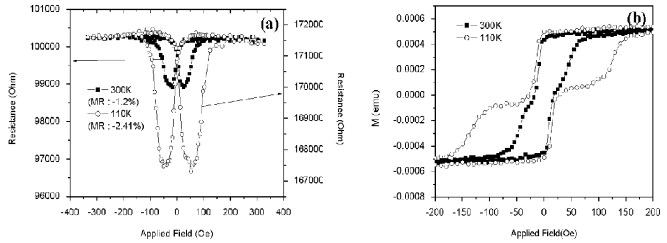

Fig. 5. Magnetoresistance transfer curve (a) of and M-H loops (b) of junction structure of Ta 3/Cu 50/Ta 3/NiFe 10/AlOx 2/Fe 1.8 nm + O_2 plasma/Fe 5/Ta 3 nm at $T = 300$ K and 110 K.

suggest that these positive MR values are likely due to existence of the Fe phase. It is reported that when Al deposits directly on top of Fe_3O_4, there will be an interface reaction, resulting in an Fe phase at the interface between Al and Fe_3O_4 layer [9]. This indicates that it is difficult to obtain a perfect Fe_3O_4 phase at the interface. For example, in the case when Fe_3O_4 was used as a bottom electrode for the MTJ, other phases such as FeO and Fe form as a result of the interface reaction when Al is deposited on top of this Fe_3O_4 layer. As seen in Fig. 3(c), the interface having mostly Fe_3O_4 and small amounts of Fe phases produces a positive MR. This means that although Fe_3O_4 may be dominant phases, a small amount of Fe can affect the MR behavior.

To show that this inverse MR curve comes from a magnetic configuration, we have measured the MR curve as well as the M-H loop at room temperature and low temperature ($T = 110$ K). This result is shown in Fig. 5. As seen in Fig. 5(a), the junction resistance increases more than 70% from 300 to 110 K. M–H loops were measured at room temperature and low temperature from the unpatterned part of the wafer. As shown in Fig. 5(b), at low temperature, the coercivity of the oxidized Fe coupled to the top Fe layer increases while the coercivity of the NiFe does not change. In our experiment, the magnetic coupling between the Fe_3O_4 and Fe was found to be ferromagnetic by measuring the moment. This M-H loop shows that the switching fields at which abrupt changes are seen in the MR curve correspond to the coercivities of the two electrodes. The magnitude of the MR is increased more than twice by the lowering of the temperature, but does not show the MR we expected from half metallic properties. Since we have succeeded in producing an Fe_3O_4 electrode in contact with the AlOx barrier, why do we not see the large MR? It is reported that MR is related to the defects and orientation of the Fe_3O_4 layer [13], [14]. The plasma-oxidized Fe in our system does not have any obvious texture but does have a lot of defects such as grain boundaries. We believe that the low MR results from defects in our polycrystalline Fe_3O_4 and possibly the existence of other phases such as FeO and γ-Fe_2O_3 at the interface.

IV. Conclusion

We have shown that by carefully controlling the oxidation condition for making Fe_3O_4 from Fe, it is possible to achieve a pure polycrystalline Fe_3O_4 interface with the AlOx barrier, resulting in an inverse MR. Small amounts of Fe lead to a positive MR.

Acknowledgment

The authors would like to thank the Data Storage Systems Center for its financial support of the research project.

This work was supported by Data Storage Systems Center at CMU.

References

[1] Ze. Zhang and S. Satpathy, "Electron states, magnetism, and the Verwey transition in magnetite," *Phys. Rev.*, vol. 44, pp. 13 319–13 331, 1991.

[2] Yu. S. Dedkov, U. Rüdiger, and G. Güntherodt, "Evidence for the half-metallic ferromagnetic state of Fe3O4 by spin-resolved photoelectron spectroscopy," *Phys. Rev. B, Condens. Matter*, vol. 65, pp. 064 417/1–064 417/5, 2002.

[3] P. M. Tedrow and R. Meservey, "Spin-dependent tunneling into ferromagnetic nickel," *Phys. Rev. Lett.*, vol. 26, pp. 192–195, 1971.

[4] M. Julliere, "Tunneling between ferromagnetic films," *Phys. Lett.*, vol. 54A, pp. 225–226, 1975.

[5] P. Sensor, A. Fert, J.-L. Maurice, F. Montaigne, F. Petroff, and A. Vaures, "Large magnetoresistance in tunnel junctions with an iron oxide electrode," *Appl. Phys. Lett.*, vol. 74, pp. 4017–4019, 1999.

[6] K.-I. Aoshima and S. X. Wang, "Fe_3O_4 and its magnetic tunneling junctions grown by ion beam deposition," *J. Appl. Phys.*, vol. 93, pp. 7954–7956, 2003.

[7] S. S. P. Parkin, X. Jiang, C. Kaiser, A. Panchula, K. Roche, and M. Samant, "Magnetically engineered spintronic sensors and memory," *Proc. IEEE.*, vol. 91, no. 10, pp. 661–680, 2003.

[8] G. Hu and Y. Suzuki, "Negative spin polarization of Fe_3O_4 in magnetite/manganite-based junctions," *Phys. Rev. Lett.*, vol. 89, p. 276 601/1-4, 2002.

[9] Y. Peng, C. Park, J. G. Zhu, R. M. White, and D. E. Laughlin, "Characterization of interfacial reactions in magnetite tunnel junctions with transmission electron microscopy," *J. Appl. Phys.*, vol. 95, pp. 6798–6800, 2004.

[10] T. B. Reed, *Free energy of formation of binary compounds: An atlas of charts for high-temperature chemical calculations*. Cambridge, MA: MIT Press, 1971.

[11] C. Park, Y. Shi, Y. Peng, K. Barmark, J. G. Zhu, D. E. Laughlin, and R. M. White, "Interfacial composition and microstructure of Fe_3O_4 magnetic tunnel junctions," *IEEE Trans. Mag.*, vol. 39, pp. 2806–2809, 2003.

[12] Y. Peng, T. Ohkubo, and D. E. Laughlin, "The investigation of nanostructures of magnetic recording media by TEM," *Scrip. Mater.*, vol. 48, pp. 937–942, 2003.

[13] X. Li, A. Gupta, G. Xiao, W. Qian, and P. David, "Fabrication and properties of heteroepitaxial magnetite (Fe_3O_4) tunnel junctions," *Appl. Phys. Lett.*, vol. 73, pp. 3282–3284, 1998.

[14] G. Hu, R. Chopdekar, and Y. Suzuki, "Observation of inverse magnetoresistance in epitaxial magnetite/manganite junctions," *J. Appl. Phys.*, vol. 93, pp. 2516–2518, 2003.

Manuscript received February 3, 2004.